From settling to rheology and hydration: How fine fractions govern the behavior of cement-based suspensions

Ahmad Khalil, Nathalie Azéma, Y. El Bitouri, G. Le Saout, S. Rémond

Powder Technology 468 (2026) 121632

Contents lists available at ScienceDirect

Powder Technology

journal homepage: www.journals.elsevier.com/powder-technology

From settling to rheology and hydration: How fine fractions govern the behavior of cement-based suspensions

A. Khalil [a], N. Azéma [a,*], Y. El Bitouri [a], G. Le Saout [a], S. Rémond [b]

[a] LMGC, IMT Mines Ales, Univ. Montpellier, CNRS, Ales, France
[b] LaMé-EA7494, Univ Orléans, Univ Tours, INSA-CVL, 8 rue Léonard De Vinci, 45072 Orléans, France

HIGHLIGHTS

- Based on granulometric analysis, identification and quantification of fine fraction of cement-based suspensions.
- How fine fraction govern settling behavior?
- Impact of fine content on rheological properties and hydration kinetics
- Experimental approach proposed to study impact of fine fraction on macroscopic behaviors in industrial suspensions.

GRAPHICAL ABSTRACT

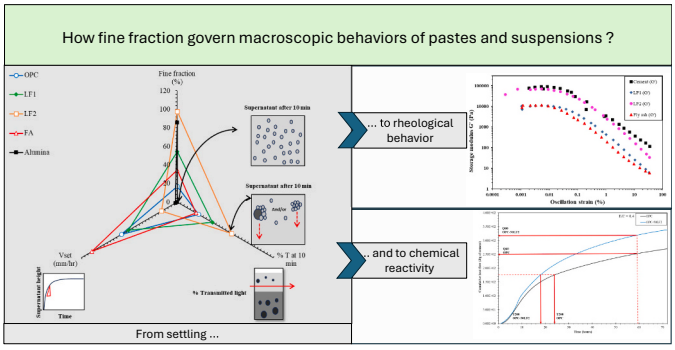

ARTICLE INFO

Keywords:
Fine particles fraction
Granular characteristics
Settling
Storage modulus
Hydration kinetics

ABSTRACT

This study investigates the role of fine particles in governing macroscopic behaviors of suspensions, in particular, cement-based pastes. Granulometric analyses were performed on both raw and binary systems of Portland cement with limestone filler re-grinded or not (LF2, LF1), and fly ash (FA) at various substitution rates (0–100 % vol) to modify fine particle content and identify a particle size threshold. Based on granulometric analyses, a threshold of 5 μm was justified and chosen for subsequent investigation. Suspension stability was assessed using Turbiscan Lab, measuring both settling velocity and supernatant clarity. The results indicate that systems with a higher fine fraction, such as those with LF2 (97.6 %), exhibit enhanced stability, as evidenced by significantly reduced settling velocity compared to LF1 (54.4 %) that demonstrates moderate stability, and FA (34.4 %) that displays pronounced instability. Rheological measurements were performed on raw and 50 % binary systems, and the results revealed that systems with a higher fine fraction exhibit a higher storage modulus G', notably LF2 compared to LF1 and FA, and OPC-50LF2 compared to OPC-50LF1 and OPC-50FA, indicating a denser structural network. Additionally, systems with a high fine fraction displayed a lower percolation threshold confirming the enhanced ability of fine particles to form interconnected networks. Isothermal calorimetry further showed that replacing 50 % of OPC with LF2 and LF1 leads to an increase in the intensity of the main hydration peak by 58 % and 47 %, respectively, compared to pure OPC, indicating that the nucleation-precipitation effect is more pronounced when more fine particles in the system.

* Corresponding author.
E-mail address: Nathalie.azema@mines-ales.fr (N. Azéma).

https://doi.org/10.1016/j.powtec.2025.121632
Received 24 July 2025; Received in revised form 4 September 2025; Accepted 5 September 2025
Available online 6 September 2025

1. Introduction

For several industrial applications, fine particles of powder materials, as raw materials or end products, and their granular characteristics govern material properties and performances. In concrete industry, given the increasing demand for cement and its expanding applications, reducing its environmental impact has become imperative. In 2022, global cement production reached approximately 4.1 billion tons, accounting for almost 8 % of global CO_2 emissions [1]. The cement industry is exploring several approaches to mitigate emissions, including the substitution of clinker with supplementary cementitious materials (SCMs) derived from minerals and industrial by-products, the use of alternative fuels from biomass, and the development of low-carbon cements containing minimal clinker content. Modern cementitious materials increasingly incorporate high levels of clinker substitution through the addition of SCMs such as fly ash, slag, silica fume, pozzolans, and limestone fillers. Their incorporation into the concrete mixture offers significant environmental and performance benefits for various cement applications such as 3D printable concrete and self-compacted concrete. Furthermore, these materials exhibit diverse reactivities, ranging from inert to pozzolanic or latent hydraulic properties, and can be either polydispersed or mono-dispersed. Their fine particles content significantly influences both the fresh and hardened states and can influence the dosage and the efficiency of chemical admixtures for cementitious materials.

In a powder or suspension, particle size is a key parameter influencing flowability, reactivity, and overall behavior [2,3]. The physical and chemical properties of particles (for reactive systems) can vary significantly with particle size, it is, thus, an important factor affecting the performance and efficacy of the final products.

The definition of “fines” can be context-dependent within related fields. In the context of aggregate classification for concrete, “fine aggregate” is characterized as particles that are smaller than 4.75 mm in diameter (No. 4) referring to ASTM C33 / EN 12620, while particles passing through the 75 μm (No. 200) sieve are categorized as “fines” or “mineral filler” referring to ASTM C117 / EN 933–1 [4]. In cement manufacturing and quality control, the fineness of the material is typically evaluated based on the amount of material retained on a 45 μm (No. 325) sieve “ASTM E11” [5]. In powder technology, ISO 12103-1 classifies the particles less than 10 μm as “Ultrafine Test Dust”, and the particles less than 80 μm as “Fine Test Dust”. This standard was initially created for testing automotive cabin air filters, illustrating such classification for specific applications [6].

In the pharmaceutical industry, fine particles which are generally micro-sized particles (1–10 μm), can impact the drug delivery and efficacy, ensuring that the drug can be effectively absorbed into the bloodstream [7]. Obviously, in soil mechanics, particles are classified according to their engineering behavior, in the case of “clay”, upper particle size limit is 2 μm, and it ranges from 2 to 63 μm in the case of “silt” [8,9].

In construction materials, fine particles are generally between 1 and 100 μm, ultrafine or submicronic particles are less than 1 μm, and recently, nano-particles are less than 0.1 μm [10]. Indeed, there is no single, accepted definition for the term “fine particles” across the different fields, which highlights the need for establishing parameters specifically relevant to cement-based materials.

In cement-based systems, variations in particle size can directly affect phenomena such as flowability, sedimentation behavior, packing density, and hydration kinetics [11–13]. For instance, fly ash, a common SCM, generally consists of spherical particles ranging from 10 to 100 μm in diameter [5]. Limestone fillers, another common addition typically have a mean particle diameter (d50) ranging from a few micrometers to coarser grades [14]. Silica fume, which belongs to a finer category of materials, contains a significant fraction of sub-micron particles and has a mean particle size of approximately 6 μm [15]. In addition, Ordinary Portland Cement OPC, usually with a mean particle size in the range of 10 to 20 μm, has a broad particle size distribution (PSD) [16]. Several studies have demonstrated that the reduction in the median particle size of fly ash in blended cement pastes leads to increased consumption of calcium hydroxide, resulting in a denser microstructure, higher heat of hydration and shortened induction period [17,18]. Similarly, the fineness of limestone has been shown to significantly affect the hydration reaction, since a higher specific surface area of limestone powder provides more nucleation sites [19] [15]. In addition, Jiang et al. [20] have demonstrated that limestone powder could accelerate the hydration reaction of cement-limestone paste due to its fine particle size. Recently, it has been proven that optimizing the particle size distribution of limestone powder can compensate for the dilution effect associated with high-volume limestone substitution (up to 50 %) [19,21]. Additionally, packing density is influenced by particle size. An optimal proportion of fine particles can enhance packing efficiency, reduce voids, and promote a denser microstructure [22].

Furthermore, physico-chemical stability is an important property for many cement-based applications, such as self-compacting concrete SCC, and 3D printable concrete. In fact, the resistance of a cement suspension against settling depends on a precise equilibrium between forces operating on the particles. Factors like PSD, shape, and density of the particles play an important role in governing the settling behavior of the suspension. Additionally, the inter-particle forces such as Van der Waals attractions, electrostatic repulsions, and additional chemical effects play also an important role alongside liquid phase properties [23]. The agglomeration of particles leads to faster settling making the suspension less stable. The DLVO theory helps explain stability by highlighting the balance between attractive Van der Waals forces and repulsive electrostatic forces [24].

Fine particles can play an important role in determining the properties of cementitious materials. This study aims to provide a fundamental understanding of how fine particles, often overlooked in traditional approaches, govern the macroscopic behavior of cement-based suspensions. However, the absence of a universal definition for fines particles required an adapted approach to define the fine fraction by selecting a reference fine powder based on the PSD of the raw powders. Consequently, the influence of fine particles fraction was then evaluated across three critical aspects: physico-chemical stability, characterized by settling velocity and supernatant clarity; rheological behavior, examined at different solid volume fractions through the evolution of storage modulus G’; and hydration kinetics, analyzed through calorimetric measurements. Furthermore, the proposed experimental approach can be extended to a broad range of particulate suspensions, both reactive and inert, such as those for ceramics, coatings, the paper industry, and cosmetics, where fine particles play an important role in determining macroscopic behavior and performance.

2. Materials and methods

The raw materials used in this study were an Ordinary Portland Cement CEM I 52.5R (OPC) supplied by Lafarge Holcim, a fly ash (FA) from Cemex, and a limestone filler, LF1, from Omya BL. We selected these three systems to cover different granularity and reactivity, as OPC the reactive one, fly ash, a moderately reactive and spherical shape, and LF1 as a quasi-inert system.

Binary cementitious systems were prepared by partially replacing Portland cement with each of the two SCMs (LF1, and FA). The volumetric replacement percentages investigated were 5 %, 25 %, 50 %, 75 %, and 95 %.

2.1. Particle size distribution

The particle size distribution (PSD) of the powders used in cementitious systems is a critical parameter that strongly influences the overall behavior [25,26]. In particular, fine particles play an important role by filling the pores between coarser particles, modifying the rheology, and

providing additional nucleation sites for cement hydration [27,28]. However, their efficiency also depends on their availability and their dispersion state. Considering the significant implications of the particle size distribution (PSD), it is important to gain a deeper understanding of the underlying physical and chemical mechanisms governing cementitious suspensions.

A well-defined measurement protocol was developed to minimize errors, ensure repeatability, and capture the "representative" distribution of fine particles. Suspensions of each powder (raw materials and binary mixtures) were prepared at a solid volume fraction of 15 %. This solid volume fraction was chosen to ensure representative sampling and consistency with conditions used for turbidimetry measurements (see section 2.5), allowing for direct comparison across different characterization techniques. A measured amount of powder was mixed with deionized water using a planetary agitator (Stuart SS30) at 500 rpm for 10 min to achieve uniform dispersion. While an alcoholic medium (isopropanol, ethanol, methanol) is preferred for cementitious powders to prevent solubilization [29] [30], this study required a different approach. As settling kinetics measurements were conducted in deionized water (section 2.5 – we can note that in presence of cement, deionized water is quickly changing into interstitial ionic liquid due to the chemical reactivity of cement), we chose to use deionized water as the carrier liquid medium for PSD analysis as well. This allows for a direct and relevant comparison between the initial particle size and the observed settling behavior. For comparative purposes, the analysis was also conducted using ethanol as carrier liquid medium, and the results are presented in Appendix. Following initial mixing, the suspension was diluted tenfold (x10) with deionized water to optimize measurement conditions for laser granulometry. The diluted sample was then subjected to further agitation using a magnetic stirrer for 5 min to maintain dispersion and prevent particles settling. PSD measurements were performed using a laser granulometer (LS 13320 Beckman Coulter). These measurements were performed in triplicate with three independently prepared suspensions for each sample to ensure repeatability and accuracy. An optical model consisting of a real part (calculated as the weighted sum of the refractive indices of components based on their percentage [31]) and an imaginary part (typically provided by the granulometer manufacturer or from literature [29]) was used for each system. The specific optical model parameters employed for each material are detailed in Appendix. The PSD of raw materials is presented in Fig. 1.

It appears that Portland cement OPC exhibits a main peak at 8.5 μm, with 50 % vol of its particles are finer than 77 μm and 98 % vol are below 23 μm. The limestone filler LF1 has a main peak at 4.9 μm, with half of its particles smaller than 5.1 μm. Fly ash, on the other hand, exhibits the broadest particle size distribution, with a main peak at 8.5 μm and 50 % vol of its particles are smaller than 9.1 μm.

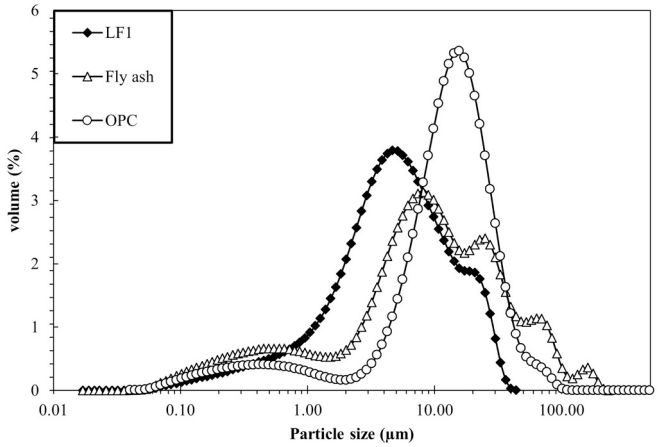

Fig. 1. Particle size distribution of raw powders.

The measurements are extended to binary systems at substitution rates of 5 %, 25 %, 50 %, 75 %, and 95 % by volume. Specifically, this investigation aims to understand the mechanisms governing granular structuration linked to agglomeration and dispersion phenomena in these systems, to control the fine particles content and highlight their role. These results are discussed in section 3.1.

2.2. SEM observations

SEM observations using Quanta 200 FEG (FEI) were performed using an adapted protocol to achieve an even dispersion of particles on a lamella. This approach is required for visualizing the morphological characteristics of raw powders [32]. The first step is to place a drop of liquid (deionized water) in the center of an ethanol-cleaned lamella, resulting in a clean, uniform surface for particle dispersion. A drop of the diluted solution (prepared in the same way as for Laser granulometric measurements) is then added to the liquid drop, ensuring that the particles are evenly distributed across the slide. To remove excess liquid, lightly touch the drop's edge with a clean, dry piece of absorbent paper. This enables selective absorption of excess liquid, allowing us to observe the granular diversity of particles/agglomerates/aggregates in the suspension.

The cement particles (Fig. 2-a,b) exhibit an angular and irregular shape with sharp edges and corners due to grinding operations. Limestone filler particles (Fig. 2-c,d), with particle shapes close to those of cement particles, reveal that the individual particles adopt a cubic crystal or prismatic grain shape. Finally, the fly ash particles (Fig. 2-e,f) are predominantly spherical with smooth surfaces, a result of the high-temperature combustion process in coal-fired power plants.

2.3. Bulk density and specific surface area

The bulk densities of the powders (raw and binary systems) are determined using a helium pycnometer "Micromeritics AccuPyc 1330". The bulk densities of binary systems were measured to assess the homogeneity of the blended mixtures. The results showed consistent values between the measured density d_{exp} and calculated density d_{calc}, determined using the volume fraction and the density of each component, across all systems with a standard deviation less than 0.1 g/cm^3, confirming its homogeneity at the macroscopic scale (Fig. 3).

Specific surface area SSA is determined using the BET method. Fly ash exhibits a relatively high specific surface area (4.69 m^2/g) compared to the other powders. The results are presented in Table 1.

2.4. Selection of the fine fraction

Limestone filler LF1, as a "quasi-inert" material with granular characteristics close to OPC, was selected to highlight the impact of fine particles without any chemical effects, while LF2 produced by grinding LF1 (90 s for each 150 g batch, using ring mill grinder) was used to modify and better control of fine content in the system. PSD measurements were conducted for LF2 powder, using the same protocol in section 2.1. The results are presented in Fig. 4. Characterization revealed that the resulting LF2 powder exhibits a main mode at 3.3 μm with half of its particles are smaller than 2.6 μm. We can also note that 97.6 % vol of particles are finer than 5 μm, which corresponds approximately to the d_{50} and main mode values for LF1. The grinding process applied to produce LF2 resulted in an even higher specific surface area of 6.79 m^2/g. The results are presented in Table 1. For these reasons, LF2 will be considered as a reference fine powder with nearly all particles finer than 5 μm. Therefore, 5 μm is adopted as a threshold to define the fine fraction in this study. Therefore, this choice of 5 μm as a threshold is not an arbitrary but a suitable criterion representing the upper boundary of our reference fines, (LF2).

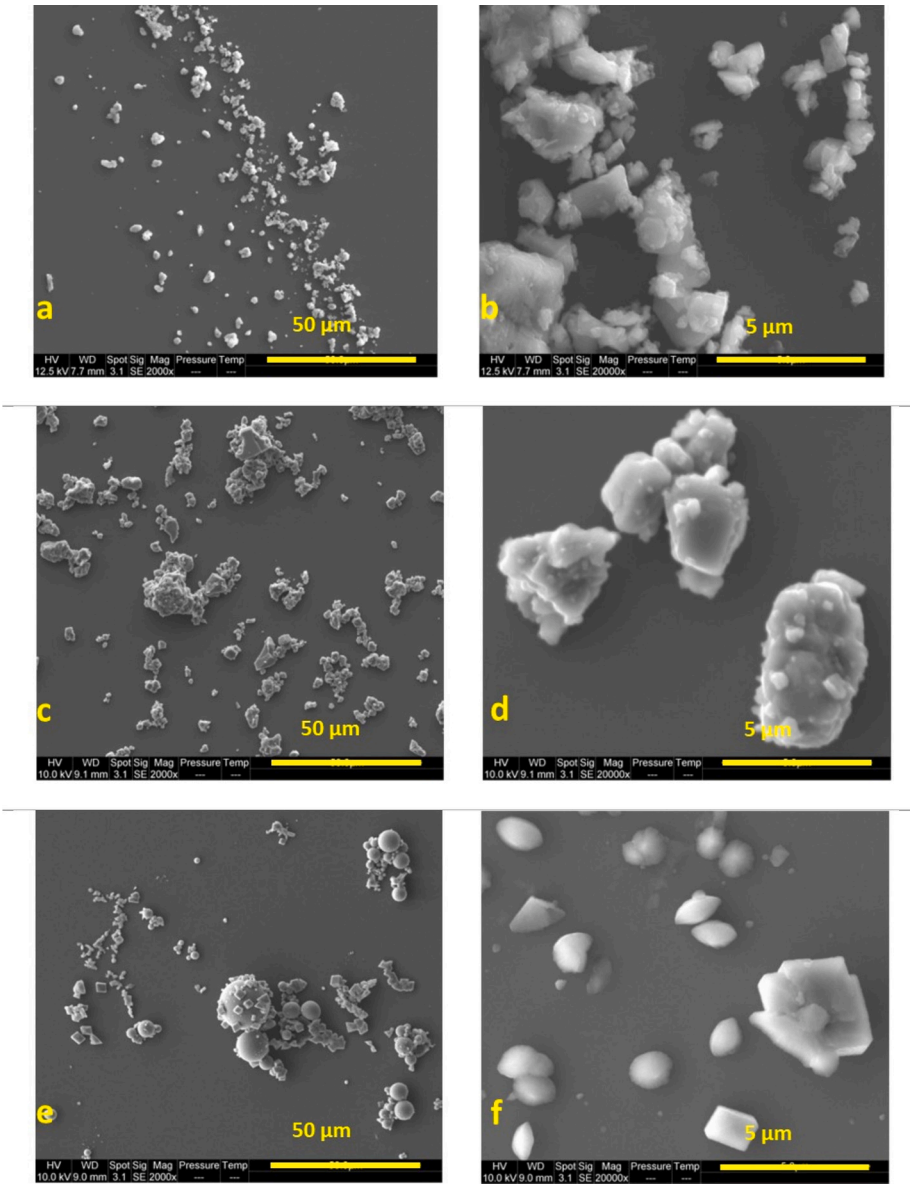

Fig. 2. SEM images of raw powders, (a; b) Cement, (c; d) LF1 and (e; f) fly ash.

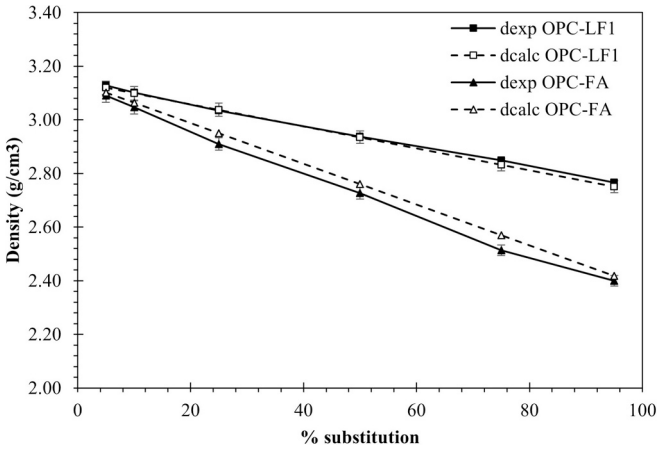

Fig. 3. Measured and calculated densities of binary systems.

Table 1
Granular characteristics of raw powders.

Material	Portland cement	LF1	LF2	Fly ash
%vol of particles <5 µm	16.9	54.4	97.6	34.4
d_2 (µm)	0.28	0.2	0.24	0.1
d_{50} (µm)	77	5.1	2.6	9.1
d_{98} (µm)	23	25	6	95
d_{mean} (µm)	8.6	7.5	2.7	18.9
Main mode (µm)	8.5	5	3.3	8.5
SSA $_{BET}$ (m^2/g)	1.43	0.99	6.79	4.69
Density (g/cm^3)	*3.14*	*2.73*	*2.73*	*2.38*

2.5. Settling kinetics measurements

Settling behavior of raw and binary systems has been monitored using a Turbiscan Lab from Microtrac-Formulaction France. This device employs a vertical light scanner with a near-infrared light source (ƛ = 860 nm) that scans the analysis tube containing the suspension sample at 40 µm intervals following a choice of specific time sequence: every 30 s during the first 3 min, then every 1 min for the next 12 min, every 5 min

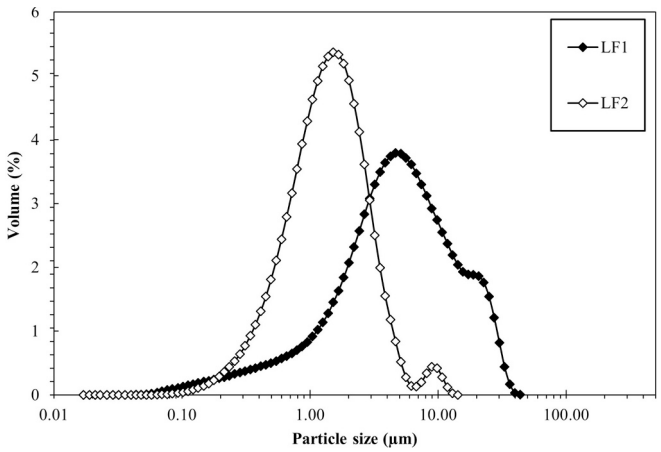

Fig. 4. PSD of limestone filler 2 (LF2).

for the subsequent 50 min, and finally every 10 min for the last 70 min. The transmitted and backscattered lights are detected at 0° and 135°, respectively, relative to the incident beam [33,34]. A suspension for each raw and binary system, with a solid volume fraction of 15 %, is prepared by mixing the amount of powders with deionized water using the same mixing protocol used for granulometric measurements (section 2.1), (10 min at a low speed (500 rpm) to ensure proper wetting of the powders and to prevent the formation of foam and air bubbles). While mixing, the analysis cell (internal diameter: 25 mm, height: 55 mm) is filled with 20 ml of the suspension using a micropipette and introduced immediately into the Turbiscan. The samples prepared are immediately analyzed, and the results are discussed in section 3.2.

Fig. 5 presents an example of a sedimentation column along with the corresponding transmission and backscattering profiles captured over time. With increasing time, the suspended particles gradually migrate toward the bottom of the cell, forming (for all systems) a sediment with a sharp front between the supernatant and the sediment formed. The turbidity of the supernatant is assessed by determining the percentage of transmitted light (%T) within the supernatant zone using the 10-min scan to determine the mean %T value. While the settling velocity (V_{set}) is determined as the slope of the evolution of sedimentation front over time. For consistency, Vset and %T are evaluated at a fixed time point, 10 min after the start of the analysis. The results will be discussed in section 3.2.

2.6. Rheological measurements

To highlight the influence of fine particles (< 5 µm) on the rheological properties, suspensions of each powder and binary blends with 50 % vol of replacement were prepared at varying solid volume fractions. Rheological measurements were conducted using a rotational rheometer (AR2000Ex from TA Instruments) equipped with a four-blade vane geometry (internal diameter: 28 mm; outer cup diameter: 30 mm). After a pre-shear phase for 30 s at a rotational shear rate of 100 s^{-1}, an oscillation strain sweep from 0.0001 % to 100 % was performed with a frequency of 1 Hz at a constant temperature of 25 °C. The typical response consists of three domains including the viscoelastic domain, the yielding domain, and the flow domain [35] [36]. The results will be discussed later in section 3.3.

2.7. Hydration kinetics measurements

The heat evolution of fresh cement-based pastes was measured using an isothermal calorimeter TAM Air (TA Instruments). Binary pastes of OPC with limestone filler (LF1 and LF2) and fly ash were prepared at substitution rates of 0 %, 5 %, 25 %, 50 %, 75 % by volume. The water to binder ratio was fixed at 0.4 for all mixtures. Approximately, 10 g of each paste were carefully transferred to glass ampoules, which were then sealed to prevent evaporation during the measurement period. The measurements were performed at a constant temperature of 25 °C.

Measurements began several minutes (about 5 min) after the moment of initial contact between deionized water and powder particles. Heat flow was recorded continuously for 72 h. Two parameters were monitored to characterize the hydration kinetics, the cumulative heat release after 60 h Q(60 h) in J/g OPC, and time required to reach a cumulative heat release of 200 J/g OPC (T200) in hours, as illustrated in Fig. 6. The impact of fine fraction on these two parameters will be discussed in section 3.4.

3. Results and discussions

3.1. Granular structuration in binary systems

Granulometric measurements were also conducted on binary systems with the same protocol (section 2.1). A comparative analysis was

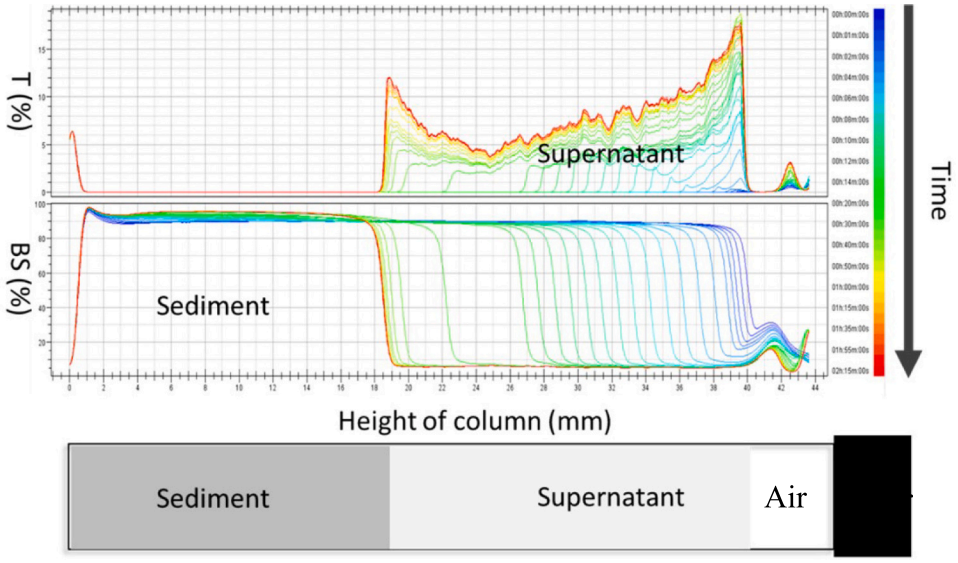

Fig. 5. Example of Turbiscan settling profiles for a cement-based suspension.

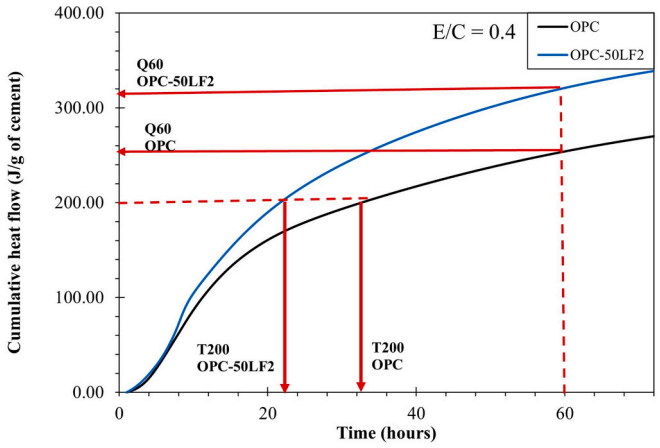

Fig. 6. Typical normalized cumulative heat release for OPC paste, E/C = 0.4, and graphical representation of followed hydration parameters.

performed between the experimental distribution (G_{exp}), measured directly by laser diffraction granulometry to capture the experimental particle size profile of the blended system, and the expected distribution (G_{calc}), calculated as a combination of each experimental distribution.

Fig. 7 illustrates an example of the two distributions (G_{exp} and G_{calc}) for the binary mixture OPC-25LF1 (75 %OPC + 25 %LF1). A close agreement is observed between the experimental and expected PSDs for the OPC-25LF1 system. Furthermore, to systematically highlights the evolution of PSD that reflects the granular modifications, four granulometric thresholds were defined within the distributions, firstly, the submicronic fraction (particles less than 1 μm) or f(1 μm), the size-gap fraction (particles less than 2 μm) or f(2 μm), the limestone-main mode fraction (particles less than 5 μm) or f(5 μm), and the OPC-main mode fraction (particles less than 10 μm) or f(10 μm). For each threshold, the experimental (f_{exp}) and calculated (f_{calc}) cumulative volume fraction of fines were determined for all binary systems. The results for the OPC-LF1 system are presented in Fig. 8.

Fig. 8 shows a strong correlation between f_{exp} and f_{calc} across all substitution rates and for all selected thresholds. It appears that for the very fine fractions f(1 μm) and f(2 μm), no significant change is observed in their evolution with increasing substitution rate. This indicates that these fine fractions are not sensitive to substitution rate and are therefore unsuitable as control parameters for the fine fraction modification. On the other hand, more significant change is observed for f(5 μm) and f (10 μm), suggesting that these thresholds are more sensitive to substitution and are more suitable for controlling and modifying the fine fraction. Consequently, for the remainder of this paper, the fine fraction is precisely defined as the particle size fraction smaller than 5 μm for all systems, with their respective values presented in Table 2.

3.2. *Influence of fine fraction on settling behavior*

The stability of cement-based suspensions is notably influenced by the complex interplay among density, particle size distribution, interparticle forces, and chemical reactivity. Sedimentation behavior or settling of particles/agglomerates occurring under gravitational force in the continuous medium is characterized, in this study, by settling velocity and the percentage of transmitted light through the supernatant after 10 min, as detailed in section 2.5.

Fig. 9 provides a comparative visualization of the stability behavior observed through the different raw powders and their fine fraction as defined above. A suspension of Alumina powder (100 % corundum, d_{50} = 2.5 μm, and f_{exp}(5 μm) = 86 %) was used for comparison demonstrating a well-dispersed system where fine particles remain suspended without significant agglomeration phenomena, sedimentation or clarification. As the fine particle fraction plays a crucial role in determining

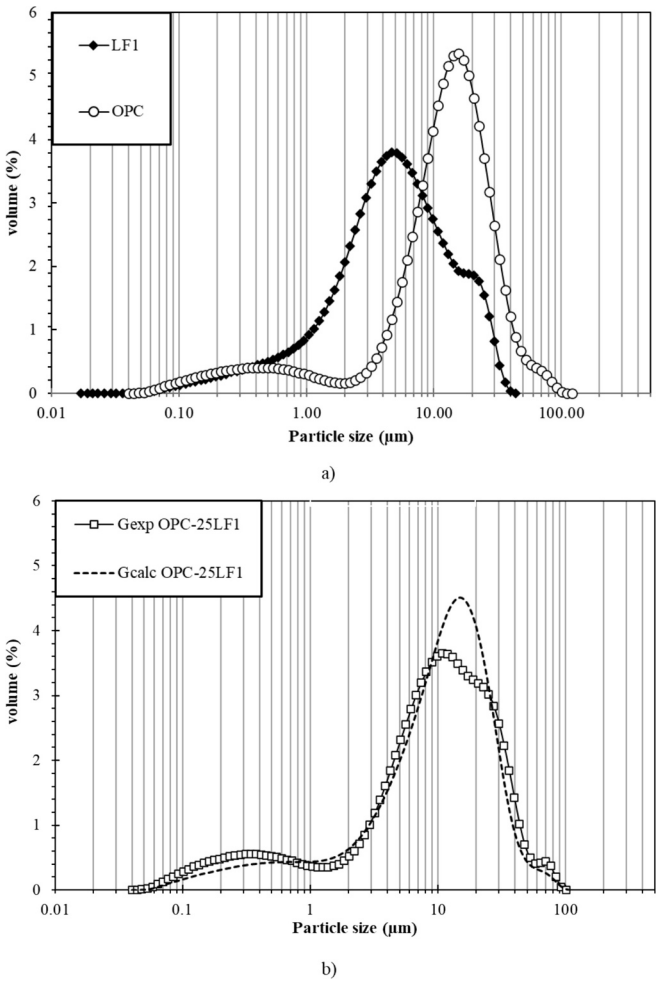

Fig. 7. Measured and expected distribution for OPC-25LF1 system (in water).

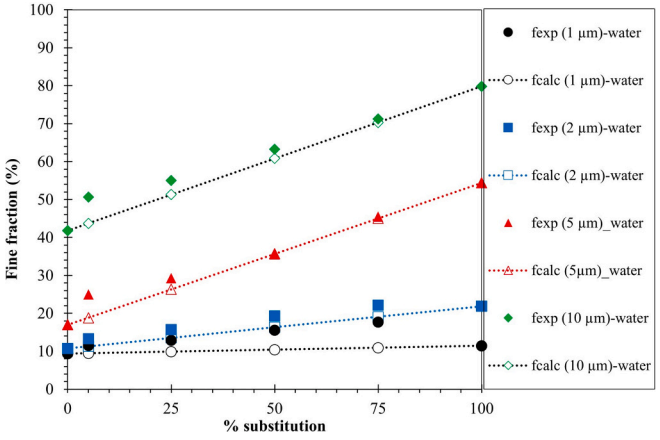

Fig. 8. Experimental and calculated fine fraction for the system OPC-LF1.

suspension stability, Alumina and LF2, with the highest fine fraction, exhibited the lowest settling velocity (2.2 and 19.6 mm/h respectively), indicating that fine particles effectively reduce gravitational settling, thereby enhancing suspension stability. However, contrary to Alumina, which shows excellent stability (without supernatant during the time analysis), LF2 displayed the supernatant with the highest %T at 10 min (68.1 %) after 10 min (low settling velocity: 19.66 mm/h). It is important to note that the supernatant height of LF2 was relatively negligible after 10 min, confirming its overall good stability despite the

Table 2
Fine fraction for raw and binary systems used for the rest of this study.

	Fine fraction (%) (< 5 μm)		
% substitution	LF1	LF2	Fly ash
0	16.9	16.9	16.9
5	18.8	20.9	17.8
25	25.3	37.1	21.3
50	35.7	57.3	25.7
75	45	77.4	30.1
95	52.5	93.6	33.6
100	54.4	97.6	34.4

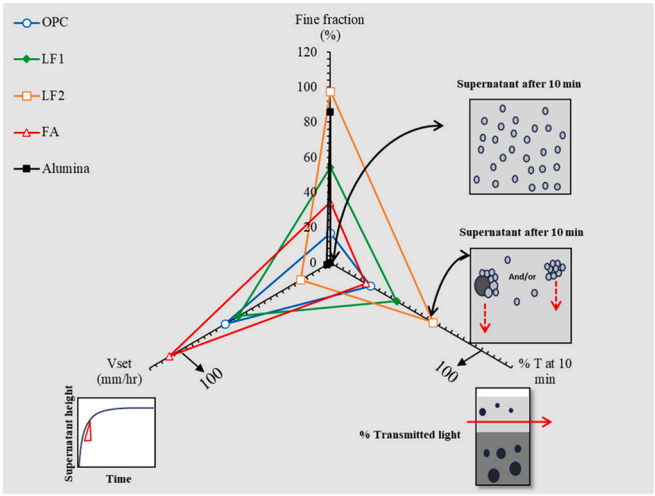

Fig. 9. Comparative stability relating the fine fraction (< 5 μm), settling velocity Vset, and supernatant clarity (%T at 10 min) for the different raw powders.

supernatant clarity. However, the presence of the supernatant suggests that, despite its low settling velocity, a small number of fine particles in LF2 might either be settling or forming loose agglomerates that allow light to pass through.

Furthermore, OPC and LF1, which both present nearly similar granular characteristics, show comparable and moderate settling velocity (69.8 and 61.1 mm/h respectively). The slight difference in V_{set} can be attributed to the difference in density, where LF1 has a lower density than OPC (2.73 and 3.14 g/cm^3 respectively) and fineness (where LF1 is finer than OPC). In these systems, "hindered settling" is the dominant mechanism. This behavior points to a balance between competing processes: partial agglomeration and coarser particles that facilitate settling, and residual dispersion that maintains fines in suspension. Nevertheless, the lower supernatant clarity for OPC (26.5 %), suggests that weakly bound agglomerates or partially dissolved cement particles (which decrease in size) may contribute to increase the turbidity of the supernatant. The lower sedimentation velocity for LF2 compared to LF1 can be attributed to the high fine fraction for LF2 resulting in a lower supernatant height at the same sedimentation time.

On the other hand, Fly Ash, with its comparatively lower fine fraction, demonstrated the highest settling velocity, reinforcing the notion that fine particles contribute to stability by slowing sedimentation. Additionally, Fly Ash also exhibited lower supernatant clarity compared to other powders. Indeed, Fly Ash particles rapidly form dense agglomerates (see Fig. 2-e) that settle quickly while leaving residual fine particles suspended that are not trapped into the agglomerates. Therefore, a partial "hindered settling" mechanism is taking place.

The influence of fine fraction on settling behavior of binary systems (5 %, 25 %, 50 %, 75 %, and 95 % of substitution) was also monitored. Fig. 10-a shows that the settling velocity for OPC-LF1 binary systems increases slightly (from 78.5 to 97.3 mm/h) with fine fraction, while the supernatant clarity remains nearly constant when increasing fine fraction (i.e. increase of LF1 content). This trend indicates moderately stable behavior due to the nearly similar granular characteristics of OPC and LF1. This also suggests that the fines from LF1 in the presence of OPC particles promote the formation of small, denser agglomerates (see Fig. 11-a) that settle faster than the individual components. However, for the binary system OPC-LF2, Fig. 10-b, shows a significant decrease of settling velocity (from 68.3 to 20.1 mm/h) when significant increasing in fine fraction (i.e. increase of LF2 content). We can note that Vset and supernatant clarity of binary systems OPC-Limestone filler show constant values when fine fraction achieves about 50 %. This may suggest a saturation point where the benefits of additional fine particles on stability become less pronounced, indicating an optimal fine particle content for achieving a stable suspension. On the other hand, OPC-FA system, Fig. 10-c, appears to be the most unstable system, with settling velocity that increase significantly and supernatant clarity relatively low and decrease dramatically. This behavior is explained by the tendency of coarser Fly Ash particles and agglomerates to settle quickly (see Fig. 11-b), while a significant portion of the fine particles (from both OPC and FA) remains suspended. These suspended fine particles are not effectively incorporated into the rapidly settling agglomerates, resulting in a highly turbid supernatant. This highlights that not all fine particles contribute equally to stability; their effectiveness is highly dependent on their interaction with other particles and their propensity to form stable networks rather than loose, rapidly settling agglomerates.

3.3. *Impact of fine fraction on the rheological properties*

The evolution of storage modulus G' for raw powders pastes (LF1, LF2, and FA) over fine fraction is illustrated in Fig. 12. At the same solid volume fraction, and at low oscillation strain (within the linear viscoelastic region LVR), LF1 and FA suspensions show lower G' comparing to LF2 suspension. This suggests that LF2 suspension has a more rigid network structure. The reason behind the greater G' of LF2 compared to LF1 lies in the difference in the fineness, as LF2 possesses a high fine fraction. Fine particles, due to their larger specific surface area, lead to an increased number of particle-particle contacts and enhanced interparticle forces (e.g., van der Waals forces, electrostatic interactions). These forces contribute to the formation of a more rigid network within the suspension resulting in a higher storage modulus. Furthermore, OPC has a high G' due to the ongoing chemical changes and cannot be compared with the inert systems. Interestingly, a clear correlation emerged between the storage modulus G' (represented by the mean value of G' within the LVR) and the fine fraction across all tested solid volume fractions for LF1, LF2, and FA systems. As shown in Fig. 12-a, LF2 with a fine fraction of about 97 %, contributes to stronger interparticle forces resulting in a more rigid network and greater G' compared to LF1 that has a fine fraction of about 54 %. Additionally, binary systems with 50 % OPC (Fig. 12-b) also show a strong correlation with fine fractions for all solid volume fractions. Consistently, systems with the highest fine fraction exhibited the highest G' values, while the system with the lowest fine fraction (FA) showed the lowest G'. This means that an increased proportion of fine particles enhances the rigidity of the network of interacting particles. In fact, the fine particles act as additional points of contact and interaction, increasing the overall connectivity and stiffness of the particle network. Moreover, it was observed that the percolation threshold, which represents the critical solid volume fraction from which the suspension exhibits a minimum rigidity (or yield stress [23]), correlated well with the fine fraction. Systems with a higher fine fraction exhibited a lower percolation threshold, meaning that a rigid network could form at a lower overall solid volume fraction. This is because the increased number of fine particles facilitates the formation of a connected pathway more easily, leading to a higher G' even at relatively lower solid concentrations. This implies that fine particles are highly efficient in building a load-bearing

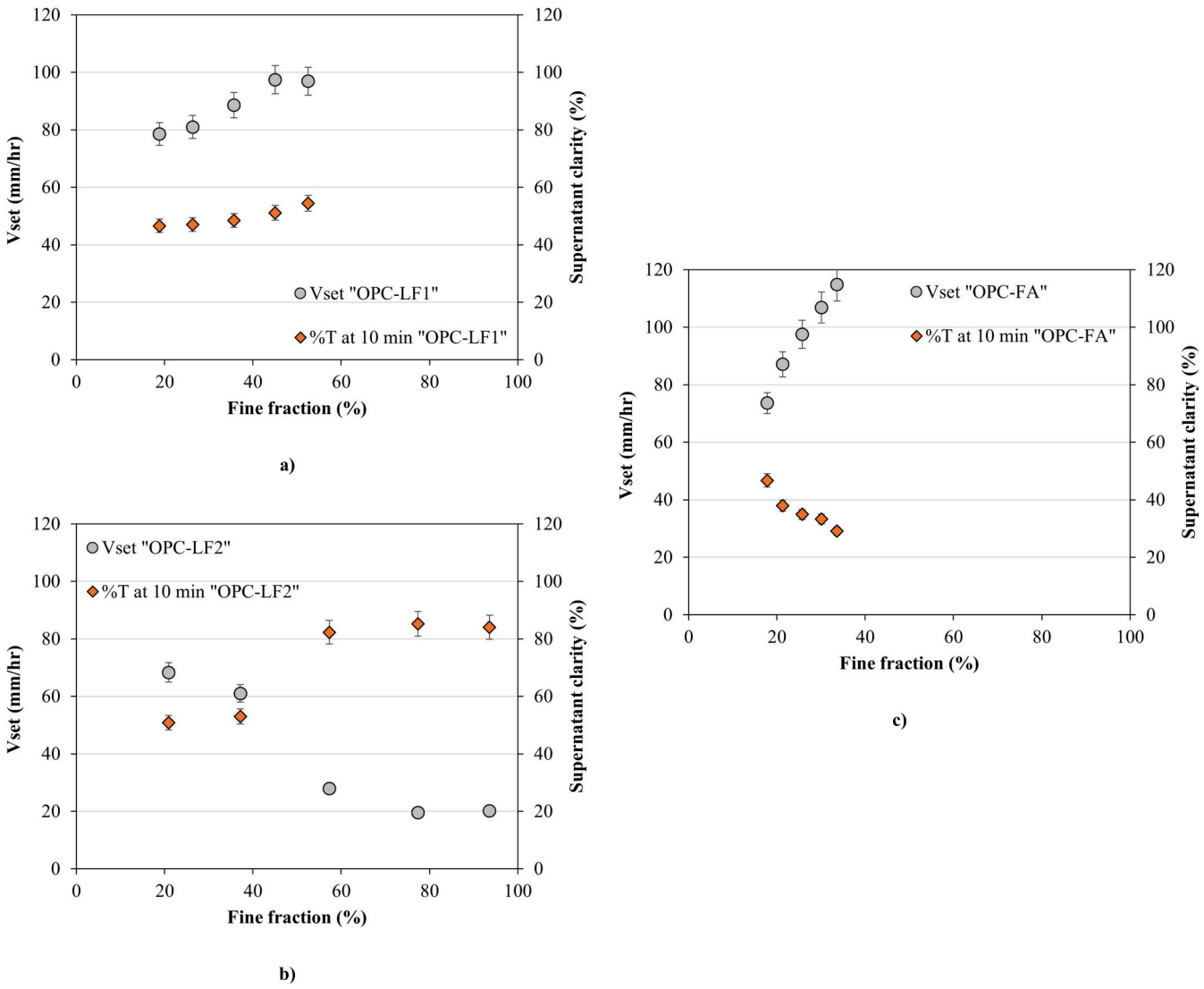

Fig. 10. Evolution of settling velocity and supernatant clarity over substitution rate for a) OPC-LF1, b) OPC-LF2, and c) OPC-FA systems.

structure within the suspension, which is crucial for applications requiring early structural integrity or shape retention, such as 3D printing of cementitious materials.

3.4. Influence of fine fraction on hydration kinetics of cement-based suspensions

The results in Fig. 13 show the heat flow evolution of cement paste with 50 % vol of limestone filler (LF1 and LF2). Following the dissolution peak (first 30 min), all systems entered in a dormant period followed by the acceleration phase which is mainly associated with the hydration of tricalcium silicate (C_3S) and the formation of calcium silicate hydrate (C-S-H), while the secondary peak is generally attributed to the hydration of aluminate phases. It was observed that the addition of limestone fillers significantly accelerates the hydration process. This acceleration effect is highly reported in literature [19,37–40]. When 50 % of OPC was replaced by limestone fillers (LF1 and LF2), a significant increase in the intensity of the peak was observed. Notably, OPC-50LF2 exhibited the highest peak intensity (5.7 mW/g of OPC) compared to about 5.3 mW/(g of OPC) for OPC-50LF1, and 3.6 mW/(g of OPC) for OPC system. This represents increases of 58 %, and 47 % for OPC-50LF2 and OPC-50LF1 respectively relative to the raw OPC system. These differences can be explained by the nucleation effect of limestone, but both limestone fillers (LF1 or LF2) are rather fine, compared to OPC particles size distribution, to create nucleation sites. Limestone particles, even if relatively coarse compared to the very fine fractions, provide additional surface area that acts as heterogeneous nucleation sites for the precipitation of hydration products, particularly C-S-H. This increased availability of nucleation sites accelerates the formation and growth of hydration products, leading to a faster overall reaction rate and thus a higher heat release rate.

In order to highlight the impact of fine fraction on hydration kinetics of cement-based pastes, T200 and Q60 were determined and plotted with the fine fraction. The results for OPC-LF1 and OPC-LF2 systems (0 %, 5 %, 25 %, 50 % and 75 % of substitution) are illustrated in Fig. 14 (a and b respectively). The cumulative heat release after 60 h (Q60), normalized to 1 g of OPC, systematically increased with increasing fine fraction (and substitution rate) for both systems. Fine particles provide additional surfaces for the heterogeneous nucleation of hydration products. According to [38], several explanations for the increased nucleation, they reported that the arrangement of the calcium atoms (resulting from the slight dissolution of limestone) on the surface of the calcite surface provides a “templating” effect which facilitate the nucleation. As we can see, this nucleation-precipitation effect is more pronounced for OPC-LF2 system, the difference here can be attributed to the difference in fineness of LF2 compared to LF1, as both share the same

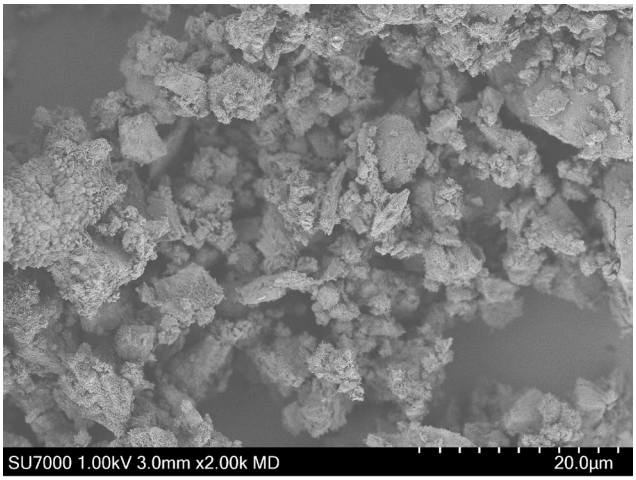

a)

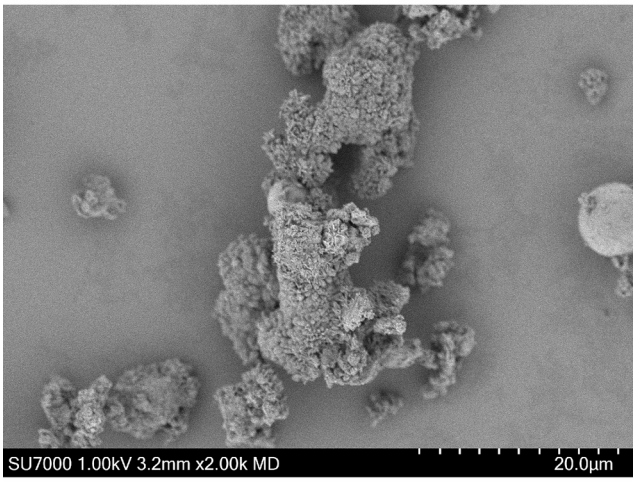

b)

Fig. 11. SEM images showing agglomeration between (a) OPC and LF1 particles; (b) OPC and FA particles.

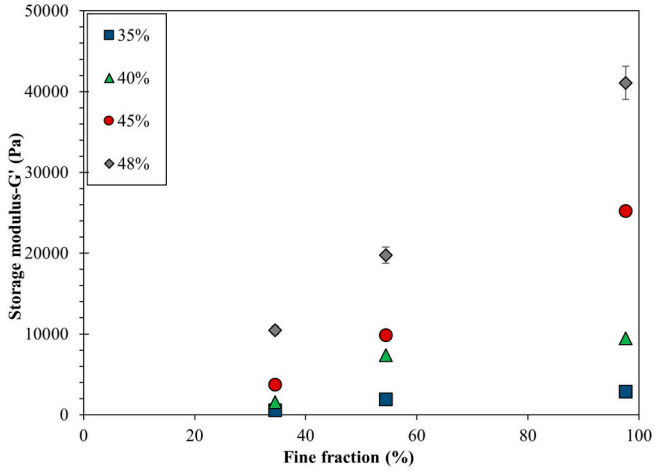

a)

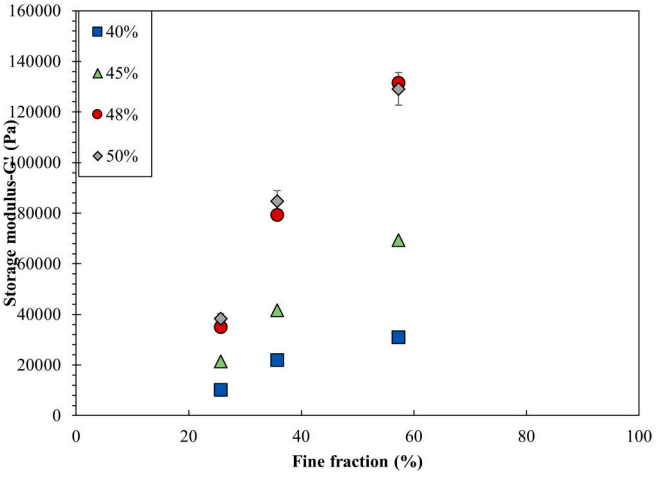

b)

Fig. 12. Evolution of storage modulus G' over fine fraction for different solid volume fraction (35 %, 40 %, 45 %, 48 %, and 50 %). (a) raw systems (LF1, LF2, and FA), (b) binary systems (OPC-50LF1, OPC-50LF2, and OPC-50FA).

chemical composition. The difference in Q60 for OPC-LF1 and OPC-LF2 is illustrated in Fig. 15. The finer particles in LF2 offer a significantly larger number of active sites for heterogeneous nucleation, leading to a more rapid and extensive formation of hydration products. Other researchers have reported that the adsorption of calcium ions (from the pore solution) on the surface of limestone particles facilitates the formation of "stable nuclei" and consequently a large amount of C-S-H nuclei on the surface of limestone particles [41]. This highlights the dual role of fine limestone particles: providing physical nucleation sites and potentially influencing the local chemistry to promote the formation of stable hydration product nuclei. The increased rate of hydration, as evidenced by higher cumulative heat release, is beneficial for applications requiring faster strength development and reduced construction times.

4. Conclusion

In this study, an approach has been developed to highlight the role of fines particles, often overlooked in traditional characterization methods,

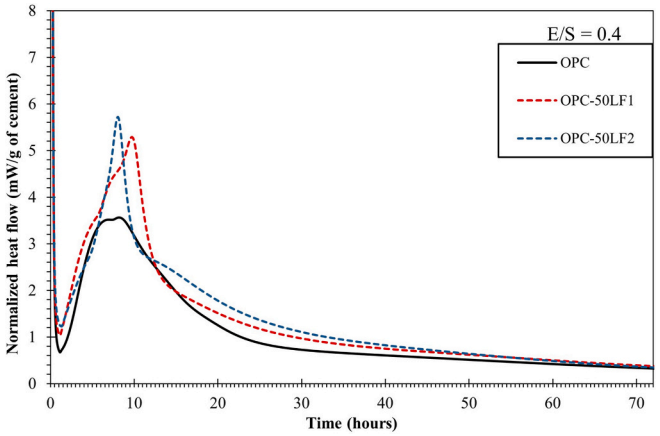

Fig. 13. Heat flow evolution of OPC, OPC-50LF1, and OPC-50LF2.

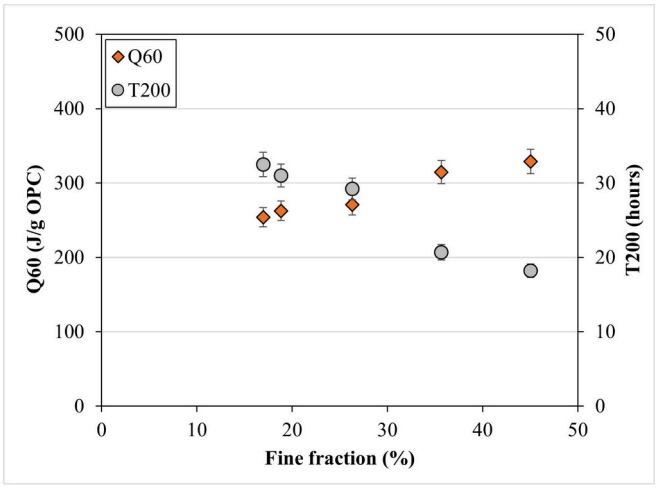

a)

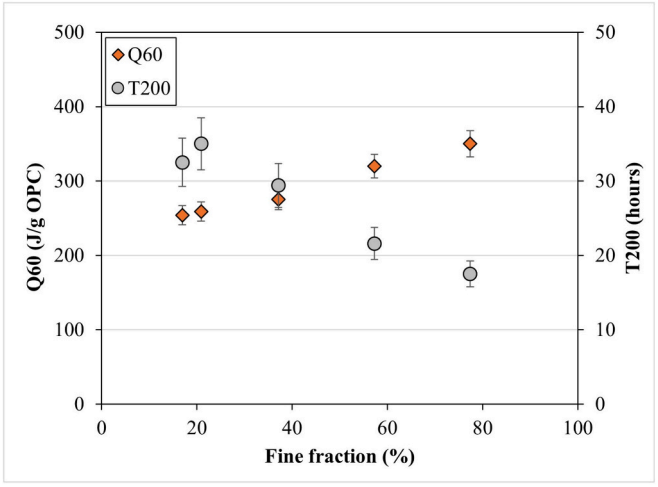

b)

Fig. 14. Evolution of Q60 and T200 with fine fraction a) OPC-LF1, and b) OPC-LF2.

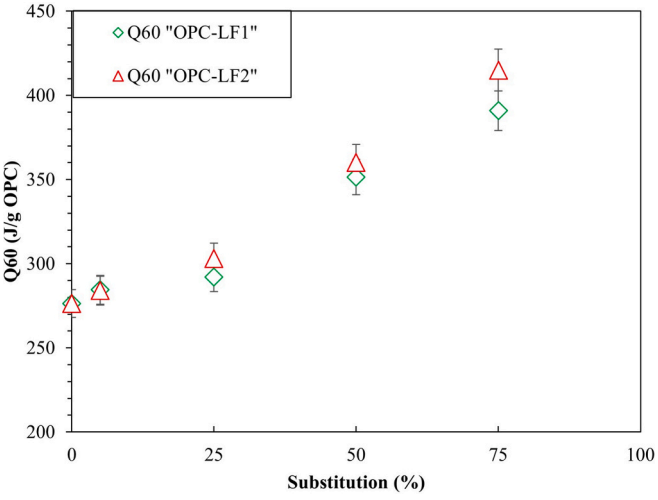

Fig. 15. Comparison of Q60 for OPC-LF1 and OPC-LF2 binary systems.

in governing the macroscopic behavior of cement-based suspensions. The absence of a universally accepted definition for fine particles in cementitious systems necessitated a careful selection of the fine particle threshold; a 5 μm threshold was chosen and rigorously justified based on comprehensive granulometric analyses across all systems. Subsequently, we highlighted the influence of fine particles fraction on three fundamental aspects relevant to advanced applications such as 3D printing and self-compacted concrete:

(i) The physico-chemical stability of the suspensions was significantly impacted by fine fraction. An increased fine particle fraction led to reduced settling behavior and enhanced supernatant clarity. This phenomenon can be attributed to several synergistic mechanisms. The larger total surface area provided by the fine particles promotes the formation of agglomerates that trapped water, effectively reducing the free water content and increasing the viscosity of the suspension.

(ii) The rheological behavior of the cement-based suspensions was markedly influenced. An increase in the fine particle fraction resulted in a significant increase in the storage modulus. This observation is primarily due to the increased particle-particle interactions. Fine particles, with their high surface area, contribute to a more extensive network within the suspension. This increased interaction leads to the formation of a more rigid and interconnected microstructure, which in turn enhances the elastic response of the material, as reflected by the higher storage modulus.

(iii) The hydration kinetics of the cementitious system were accelerated. An increased fine particle fraction induced an increase in the cumulative heat flow, indicative of enhanced nucleation-precipitation. Fine particles provide a significantly larger number of nucleation sites for the precipitation of hydration products. This increased surface area acts as a template for the heterogeneous nucleation of calcium-silicate-hydrate (C-S-H) and other phases, thereby accelerating the overall hydration process. The proximity of these nucleation sites also facilitates the rapid growth of hydration products, leading to a more efficient consumption of reactants.

Beyond their typical function as fillers, these results collectively highlight the critical role that fines particles, and their critical dosage can play in controlling the macroscopic behavior of cement-based suspensions. For instance, in 3D printing, the enhanced physico-chemical stability and increased storage modulus provided by fine particles are important for maintaining shape accuracy and preventing collapse during layer-by-layer deposition. Similarly, in self-compacted concrete, the improved stability and rheological properties ensure flowability without segregation, while the enhanced hydration contributes to early strength development and reduced formwork pressure.

CRediT authorship contribution statement

A. Khalil: Writing – original draft, Validation, Supervision, Methodology, Investigation. **N. Azéma:** Writing - original draft, Validation, Supervision, Methodology, Investigation. **Y. El Bitouri:** Writing – original draft, Validation, Supervision, Methodology, Investigation. **G. Le Saout:** Writing – original draft, Validation, Supervision, Methodology, Investigation. **S. Rémond:** Writing – original draft, Validation, Supervision, Methodology, Investigation.

Declaration of competing interest

None.

Appendix A

A.1. PSD of cementitious suspensions

A.1.1. Determination of the refractive index for the studied systems

There are 3 fixed wavelengths for PIDS: L1 = 450 nm, L2 = 600 nm, and L3 = 900 nm (Laser granulometer supplier). For each system, a specific model was created with 3 different refractive indices corresponding to each wavelength.

For binary mixtures, the following expression [42] is used to calculate the refractive index:

$$n = \sum mi*ni$$

Where:

- n: refractive index,
- mi: masse percentage of element i,
- ni: refractive index of element i.

Appendix B

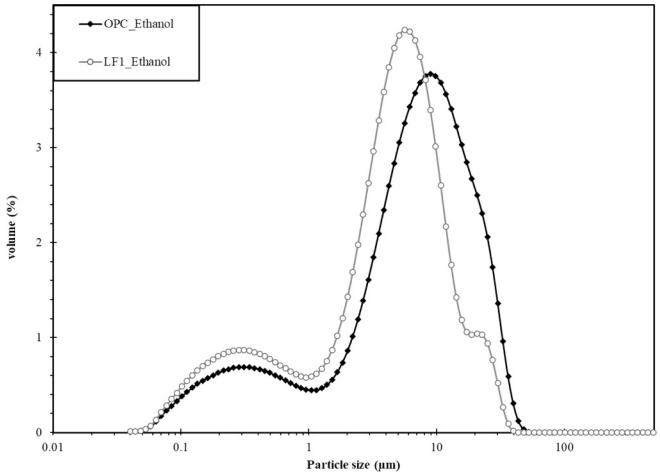

Fig. 16. PSD of OPC and LF1 using ethanol as a suspended medium

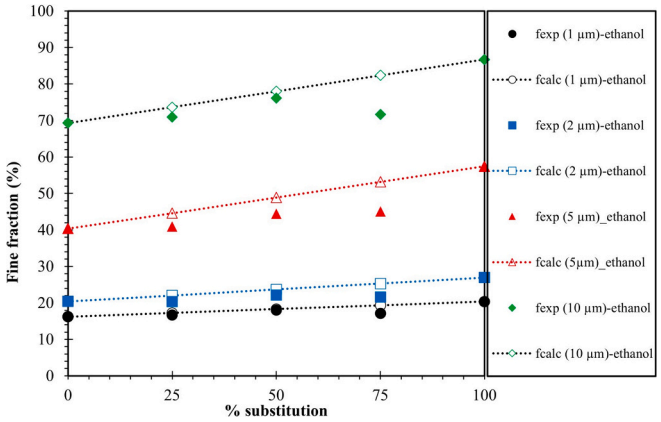

Fig. 17. Evolution of experimental and calculated fine fraction over substitution rate. Ethanol is used as a suspended medium.

Table 3
Refractive index (real part) at wavelength 450 nm.

Substitution rate (%vol)	OPC-LF	OPC-FA
0	1.75	1.75
5	1.747	1.742
25	1.732	1.71
50	1.714	1.665
75	1.694	1.612

(*continued on next page*)

Table 3 (*continued*)

Substitution rate (%vol)	OPC-LF	OPC-FA
95	1.676	1.565
100	1.672	1.552

Table 4
Refractive index (real part) at wavelength 600 nm.

Substitution rate (%vol)	OPC-LF	OPC-FA
0	1.752	1.752
5	1.748	1.744
25	1.731	1.71
50	1.708	1.662
75	1.683	1.607
95	1.662	1.557
100	1.657	1.543

Table 5
Refractive index (real part) at wavelength 900 nm.

Substitution rate (%vol)	OPC-LF	OPC-FA
0	1.754	1.754
5	1.749	1.746
25	1.730	1.71
50	1.704	1.66
75	1.676	1.603
95	1.652	1.55
100	1.646	1.536

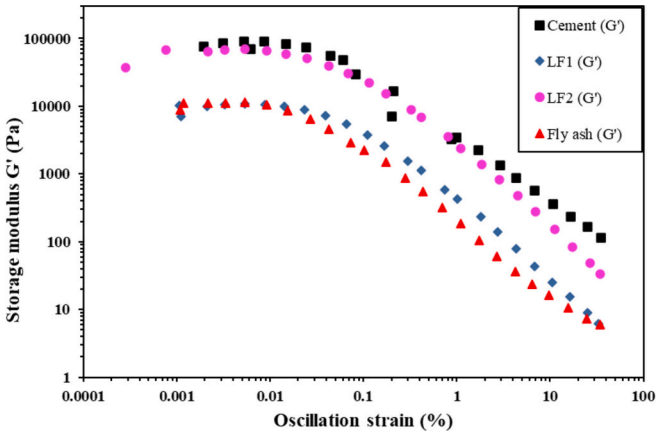

Fig. 18. Evolution of storage modulus G' over strain for pastes at a solid volume fraction of 48 %.

Data availability

Data will be made available on request.

References

[1] https://www.cembureau.eu/.
[2] Y. Kudo, M. Yasuda, S. Matsusaka, Effect of particle size distribution on flowability of granulated lactose, Adv. Powder Technol. 31 (1) (Jan. 2020) 121–127, https://doi.org/10.1016/j.apt.2019.10.004.
[3] R. Suhag, A. Kellil, M. Razem, Factors influencing food powder Flowability, Powders 3 (1) (2024) 65–76, https://doi.org/10.3390/powders3010006.
[4] Sieve Sizes: A guide to U.S. and metric sizes. GlobalGilson.com n.d. https://www.globalgilson.com/blog/sieve-sizes.
[5] Chapter 1 - Fly Ash - An Engineering material - Fly Ash Facts for Highway Engineers - Recycling - Sustainability - Pavements - Federal Highway Administration. n.d. https://www.fhwa.dot.gov/pavement/recycling/fach01.cfm.
[6] https://www.powdertechnologyinc.com/test-dust-history/iso-standard-12103-1/.
[7] N. Rasenack, B.W. Müller, Micron-size drug particles: Common and Novel Micronization Techniques, 2004, https://doi.org/10.1081/PDT-120027417.
[8] https://www.tensarinternational.com/resources/articles/what-is-particle-size-distribution-in-soils.
[9] V.J. Kilmer, L.T. Alexander, Methods of making mechanical analysis of soils, Soil Sci. 68 (1) (1949) [Online]. Available: https://journals.lww.com/soilsci/fulltext/1949/07000/methods_of_making_mechanical_analyses_of_soils.3.aspx.
[10] N. Joudeh, D. Linke, Nanoparticle classification, physicochemical properties, characterization, and applications: a comprehensive review for biologists, BioMed Central Ltd. (Dec. 01, 2022), https://doi.org/10.1186/s12951-022-01477-8.
[11] X. Ouyang, L. Yu, L. Wang, S. Xu, Y. Ma, J. Fu, Surface properties of ceramic waste powder and its effect on the rheology, hydration and strength development of cement paste, J. Build. Eng. 61 (Dec. 2022), https://doi.org/10.1016/j.jobe.2022.105253.
[12] F. Han, H. Zhang, Z. Li, Z. Pang, Effect of the fineness of limestone powder on the properties of calcium sulfoaluminate cement, J. Therm. Anal. Calorim. 148 (10) (May 2023) 4033–4047, https://doi.org/10.1007/s10973-023-12040-4.

[13] X. Hu, C. Shi, G. Ye, G. De Schutter, The influences of ultra-fine limestone powder on zeta potential of freshly mixed cement paste [Online]. Available: https://api.semanticscholar.org/CorpusID:139566785, 2016.
[14] E.K. Anastasiou, Effect of high calcium fly ash, ladle furnace slag, and limestone filler on packing density, consistency, and strength of cement pastes, Materials 14 (2) (Jan. 2021) 1–13, https://doi.org/10.3390/ma14020301.
[15] G.D. Moon, S. Oh, S.H. Jung, Y.C. Choi, Effects of the fineness of limestone powder and cement on the hydration and strength development of PLC concrete, Constr. Build. Mater. 135 (Mar. 2017) 129–136, https://doi.org/10.1016/j.conbuildmat.2016.12.189.
[16] S.R. Rajagopalan, B.Y. Lee, S.T. Kang, Prediction of the rheological properties of fresh cementitious suspensions considering microstructural parameters, Materials 15 (20) (Oct. 2022), https://doi.org/10.3390/ma15207044.
[17] F. Moghaddam, V. Sirivivatnanon, K. Vessalas, The effect of fly ash fineness on heat of hydration, microstructure, flow and compressive strength of blended cement pastes, Case Stud. Constr. Mater. 10 (Jun. 2019), https://doi.org/10.1016/j.cscm.2019.e00218.
[18] H. Li, L. Yang, Y. Xie, Effect of fineness on the properties of cement paste, Key Eng. Mater. 629–630 (Apr. 2014) 366–370, https://doi.org/10.4028/www.scientific.net/KEM.629-630.366.
[19] T. Oey, A. Kumar, J.W. Bullard, N. Neithalath, G. Sant, The filler effect: the influence of filler content and surface area on cementitious reaction rates, J. Am. Ceram. Soc. 96 (6) (Jun. 2013) 1978–1990, https://doi.org/10.1111/jace.12264.
[20] D. Jiang, et al., Utilization of limestone powder and fly ash in blended cement: rheology, strength and hydration characteristics, Constr. Build. Mater. 232 (Jan. 2020), https://doi.org/10.1016/j.conbuildmat.2019.117228.
[21] M. Marinković, A. Radović, V. Carević, Carbonation of limestone powder concrete: state-of-the-art overview, Gradjevinski materijali i konstrukcije 66 (2) (2023) 127–139, https://doi.org/10.5937/grmk2300005m.
[22] P. Zhu, et al., Cement with high-volume limestone powder: effect of powder fineness on packing density, strength and hydration behaviour, Adv. Cem. Res. 34 (7) (2021) 311–323, https://doi.org/10.1680/jadcr.21.00127.
[23] N. Roussel, A. Lemaître, R.J. Flatt, P. Coussot, Steady state flow of cement suspensions: a micromechanical state of the art, Cem. Concr. Res. 40 (1) (Jan. 2010) 77–84, https://doi.org/10.1016/j.cemconres.2009.08.026.
[24] R. Silva, F.A.P. Garcia, P.M.G.M. Faia, M.G. Rasteiro, Settling suspensions flow modelling: A review, in: Hosokawa Powder Technology Foundation, 2015, https://doi.org/10.14356/kona.2015009.
[25] D.P. Bentz, C.F. Ferraris, M.A. Galler, A.S. Hansen, J.M. Guynn, Influence of particle size distributions on yield stress and viscosity of cement-fly ash pastes, Cem. Concr. Res. 42 (2) (2012) 404–409, https://doi.org/10.1016/j.cemconres.2011.11.006.
[26] I. Mehdipour, K.H. Khayat, Effect of particle-size distribution and specific surface area of different binder systems on packing density and flow characteristics of cement paste, Cem. Concr. Compos. 78 (Apr. 2017) 120–131, https://doi.org/10.1016/j.cemconcomp.2017.01.005.
[27] Y. Knop, A. Peled, R. Cohen, Influences of limestone particle size distributions and contents on blended cement properties, Constr. Build. Mater. 71 (2014) 26–34, https://doi.org/10.1016/j.conbuildmat.2014.08.004.
[28] X. Chateau, Particle packing and the rheology of concrete, in: Understanding the Rheology of Concrete, Elsevier, 2012, pp. 117–143, https://doi.org/10.1533/9780857095282.2.117.
[29] Martin Cyr, Contribution à la caractérisation des fines minérales et à la compréhension de leur rôle joué dans le comportement rhéologique des matrices cimentaires. Matériaux. INSA de Toulouse; Université de Sherbrooke Français. ⟨NNT : ⟩. ⟨tel-00489599⟩ 1999. https://theses.hal.science/tel-00489599v1.
[30] V.A. Hackley, Analysis of the ASTM Round-Robin Test on Particle Size Distribution of Portland Cement: Phase II [Online]. Available: https://www.researchgate.net/publication/252553574, 2002.
[31] R. Reiver, N.L.S. Azema Gwenn, Étude des principaux modes d'action de molécules accélératrices sur ciments composés. http://www.theses.fr/2021EMAL0002/document, 2021.
[32] C. Autier, N. Azema, J.M. Taulemesse, L. Clerc, Mesostructure evolution of cement pastes with addition of superplasticizers highlighted by dispersion indices, Powder Technol. 249 (Nov. 2013) 282–289, https://doi.org/10.1016/j.powtec.2013.08.036.
[33] Y. El Bitouri, N. Azéma, Contribution of turbidimetry on the characterisation of cement pastes bleeding, Adv. Cem. Res. (Aug. 2022) 1–11, https://doi.org/10.1680/jadcr.22.00040.
[34] O. Mengual, G. Meunier, I. Cayre, K. Puech, P. Snabre, Characterisation of instability of concentrated dispersions by a new optical analyser: the TURBISCAN MA 1000, Colloids Surf. A Physicochem. Eng. Asp. 152 (1–2) (1999) 111–123, https://doi.org/10.1016/S0927-7757(98)00680-3.
[35] Y. El Bitouri, Deformation capacity of fresh cement pastes, Korea Aust. Rheol. J. (2024), https://doi.org/10.1007/s13367-024-00090-5.
[36] A.M. Mostafa, A. Yahia, New approach to assess build-up of cement-based suspensions, Cem. Concr. Res. 85 (Jul. 2016) 174–182, https://doi.org/10.1016/j.cemconres.2016.03.005.
[37] A.M. Poppe, G. De Schutter, Cement hydration in the presence of high filler contents, Cem. Concr. Res. 35 (12) (Dec. 2005) 2290–2299, https://doi.org/10.1016/j.cemconres.2005.03.008.
[38] E. Berodier, K. Scrivener, Understanding the filler effect on the nucleation and growth of C-S-H, J. Am. Ceram. Soc. 97 (12) (2014) 3764–3773, https://doi.org/10.1111/jace.13177.
[39] K. Scrivener, A. Ouzia, P. Juilland, A. Kunhi Mohamed, Advances in understanding cement hydration mechanisms, Elsevier Ltd, Oct. 01, 2019, https://doi.org/10.1016/j.cemconres.2019.105823.
[40] E.H. Kadri, S. Aggoun, G. De Schutter, K. Ezziane, Combined effect of chemical nature and fineness of mineral powders on Portland cement hydration, Mater. Struct./Materiaux et Constructions 43 (5) (Jun. 2010) 665–673, https://doi.org/10.1617/s11527-009-9519-6.
[41] X. Ouyang, D.A. Koleva, G. Ye, K. van Breugel, Insights into the mechanisms of nucleation and growth of C–S–H on fillers, Mater. Struct./Materiaux et Constructions 50 (5) (Oct. 2017), https://doi.org/10.1617/s11527-017-1082-y.
[42] M. Cyr, A. Tagnit-Hamou, Particle size distribution of fine powders by LASER diffraction spectrometry. Case of cementitious materials, Mater. Struct./Materiaux et Constructions 34 (6) (2001) 342–350, https://doi.org/10.1007/bf02486485.